Fractal patterns in riverbed morphology produce fractal scaling of water storage times.

A. F. Aubeneau[1], R. Martin[2], D. Bolster[1], R. Schumer[3], D. Jerolmack[4] , and A. Packman[5]

Corresponding author: A. F. Aubeneau, Department of Civil and Environmental Engineering, University of Notre Dame, Fitzpatrick Hall, Notre Dame, IN 46556, USA. (aubeneau@gmail.com)

[1]Department of Civil and Environmental Engineering, University of Notre Dame, Notre Dame, Indiana, USA.

[2]Department of Atmospheric and Oceanic Sciences, University of California Los Angeles, Los Angeles, California,USA .

[3]Division of Hydrologic Sciences, Desert Research Institute, Reno, Nevada, USA.

[4]Department of Earth and Environmental Science, University of Pennsylvania, Philadelphia, Pennsylvania, USA

This article has been accepted for publication and undergone full peer review but has not been through the copyediting, typesetting, pagination and proofreading process, which may lead to differences between this version and the Version of Record. Please cite this article as doi: 10.1002/2015GL064155

River topography is famously fractal, and the fractality of the sediment bed-surface can produce scaling in solute residence time distributions. Empirical evidence showing the relationship between fractal bed-topography and scaling of hyporheic travel-times is still lacking. We performed experiments to make high resolution observations of streambed topography and solute transport over naturally-formed sand bedforms in a large laboratory flume. We analyzed the results using both numerical and theoretical models. We found that fractal properties of the bed topography do indeed affect solute residence time distributions. Overall, our experimental, numerical and theoretical results provide evidence for a coupling between the sand-bed topography and the anomalous transport scaling in rivers. Larger bedforms induced greater hyporheic exchange and faster porewater turn-over relative to smaller bedforms, suggesting that the structure of legacy morphology may be more important to solute and contaminant transport in streams and rivers than previously recognized.

[5]Department of Civil and Environmental Engineering, Northwestern University, Evanston, Illinois, USA.

1. Introduction

Transit time distributions in rivers control the opportunity for biological uptake and transformation of a variety of critical constituents, including nitrogen, phosphorus, carbon and toxic contaminants [*Alexander et al.*, 2000; *Battin et al.*, 2003, 2008; *Raymond et al.*, 2013; *Marzadri et al.*, 2014]. Travel times in rivers and watersheds are very broadly distributed [*Kirchner et al.*, 2000; *Haggerty et al.*, 2002; *Stonedahl et al.*, 2012; *Aubeneau et al.*, 2014], but the mechanisms that produce travel time distributions over many orders of magnitude are not known precisely [*Boano et al.*, 2014]. The exchange of water between surface and subsurface flows, generally termed hyporheic exchange, plays a critical role in structuring fluvial ecosystems [*Boulton et al.*, 1998; *Aubeneau et al.*, 2015]. Several studies have shown that fractal topography can produce scaling in hyporheic residence time distributions [*Stonedahl et al.*, 2012, 2013; *Gomez-Velez and Harvey*, 2014]. *Worman et al.* [2006, 2007] used numerical experiments to demonstrate the link between fractal topography and water storage times. However, empirical evidence of this relationship is still lacking as prior studies have not resolved both channel morphology and solute transport directly over a sufficiently wide range of scales. Here we obtained high-resolution observations of streambed topography and long-term measurements of solute washout in a large laboratory flume. We found that fractal bed topography produced fractal scaling in both hyporheic residence time distributions and whole-system transit time distributions. This work firmly establishes the link between fractal geometry and fractal storage time distributions in rivers.

Large-scale river topography generally forms during floods and persists under low flow (baseflow). Reworking of sediment deposits over long periods of time produces a broad mosaic of morphological features that exhibit fractality over scales ranging from the size of clusters of individual sediment grains to entire river valleys and networks [*Nikora et al.*, 1997; *Turcotte*, 1997; *Rodriguez-Iturbe and Rinaldo*, 2001; *Jerolmack and Mohrig*, 2005]. These features create elevation gradients that induce subsurface flows [*Toth*, 1963]. In the present work, larger bedforms induced faster porewater turnover (greater fractional-in-time scaling exponents), indicating that legacy morphological structures produced during periods of high flow could influence storage timescales during low flow. Large-scale legacy morphology may therefore be more important to nutrient, carbon, and contaminant dynamics in rivers than previously recognized.

Since rivers have fractal topography and interactions between river flow and boundary topography drive hyporheic exchange[*Harvey and Bencala*, 1993; *Stonedahl et al.*, 2010; *Tonina and Buffington*, 2011; *Kiel and Cardenas*, 2014; *Gomez-Velez and Harvey*, 2014], the ubiquitous fractal properties of rivers should produce fractal patterns in hyporheic flowpaths and fractal scaling in the associated residence time distributions [*Worman et al.*, 2007; *Stonedahl et al.*, 2012]. Other mechanisms that can produce broad travel time distributions include subsurface heterogeneity and nested flowpaths in homogenuous systems [*Kirchner et al.*, 2001; *Scher et al.*, 2002; *Cardenas*, 2007]. Therefore, fractal topography may not be a necessary condition for anomalous hyporheic transport. However, no studies to date have conclusively demonstrated the link between fractal topogragraphy and subsurface residence time scaling because no available datasets include sufficient multiscale observations of both river morphology and travel times.

Thus we ask: Does fractality in bed surface morphology directly produce fractality in river transit time distributions? And do greater variations in bed surface elevations produce broader hyporheic residence time distributions? To answer these questions, we obtained high-resolution observations of streambed topography and solute transport with naturally-formed fractal bedform morphology in a large laboratory flume. We simulated hyporheic exchange and transit times through the system based on velocity fields estimated from the observed topography and streamflow conditions. We synthesized the experimental and numerical results by linking observed tracer washout curves to hyporheic residence time distributions and whole-stream transit time distributions using stochastic mobile-immobile theory [*Schumer et al.*, 2003], and relating scaling in the travel time distributions to the distribution of vertical velocities at the sediment-water interface.

2. Methods

2.1. Bed morphology and tracer washout experiment

We conducted a series of experiments in a tilting-bed flume. The flume is 15 m long, 0.9 m wide and 0.65 m deep. It was filled with 0.37 mm sand (D_{50} measured with a Retsch Camsizer) to a depth of 20 cm and adjusted to zero slope. Water discharge was controlled by a hydraulic valve and sediments were recirculated to maintain constant volume in the flume. Sediment depth was maintained by a porous wall at the downstream end of the flume. Constant water depth was maintained by a tailgate. To avoid boundary effects, we restricted data collection from 5 to 13 m from the inlet (see *Martin and Jerolmack* [2013] for more details of experimental setup).

We carried out two tracer washout experiments, one with smaller bedforms and one with larger bedforms. Bed topography was generated by a steady water discharge. In the first case, a discharge of 40 $L.s^{-1}$ (velocity $\sim$ 0.2 $m.s^{-1}$) generated bedforms 6 cm high on average (with amplitudes up to 10 cm) and 66cm long; in the second, a discharge of 80 $L.s^{-1}$ (velocity $\sim$ 0.4 $m.s^{-1}$) produced bedforms 10 cm high on average (with amplitudes up to 20 cm) and 90 cm long (see Fig.1). After sonar scans (JSR Ultrasonic DPR300 Pulser/Receive) indicated bed topography had reached a statistical steady state, we stopped flow and drained the flume slowly to gather high resolution (4 mm^2 pixels) bed topography data with a laser scanner (Keyence LKG502, see *Martin and Jerolmack* [2013]). Once the laser scans were completed, we restarted flow, filling the flume with water containing rhodamine dye at a concentration of 100 $mg.L^{-1}$. When the flume was completely filled and the flume-bed saturated with dye, we switched back to clean water. We observed the tracer release from the bed into the water column by monitoring fluorescence 13 m downstream of the inlet for over 15 hours at a 2 second sampling rate using a Turner Designs 10AU fluorometer. We refer to the obtained breakthrough curves as “washout curves” to emphasize the unusual initial condition where the bed sediment is loaded with tracer, which greatly improves resolution of tracer concentrations compared to traditional in-stream injections. A steady discharge of 20 $L.s^{-1}$ (velocity $<$0.1 $m.s^{-1}$) was maintained during the washout experiment. This was below the threshold for sediment transport, and we verified this by laser-scanning the entire bed surface topography before and after each experiment, and by monitoring longitudinal elevation transects during the injections with sonar.

2.2. Data analysis and modeling

To numerically model washout curves, we conducted a series of particle tracking simulations. First, we used surface elevation data to compute the subsurface flow field following the methods of *Worman et al.* [2006]. This spectral model performs a Fourier fit to the topography, and calculates the boundary head at the bed surface from rescaled and shifted Fourier coefficients. We then solved Laplace's equation to obtain the head distribution in the subsurface, and Darcy's law to generate the porewater flow field. For the surface flow, we imposed a logarithmic vertical velocity profile and Poiseuille flow in the x-y plane (x being the streamwise direction), although the predicted washout curves were found to be insensitive to the specific structure of the surface flow, indicating that the late-time solute behavior was entirely controlled by subsurface transport. We then performed particle-tracking simulations using these flowfields with initial conditions reflecting the experimental setup: homogeneous and uniform tracer concentration throughout the subsurface and zero tracer in the surface water. Washout curves were generated by recording the number of virtual tracer particles crossing the downstream sampling location at any time.

Additionally, we calculated topographical power spectra from the bed surface elevation data following *Turcotte* [1997] and *Rodriguez-Iturbe and Rinaldo* [2001]. The elevation spectrum (S) is defined as the squared Fourier transform $F_z(f)$ of an elevation transect z(x) such that $S(f) = F_z(f)^2$, where f is the frequency. The power spectra along all measured downstream transects were averaged to yield the results in Figure 2.

To understand how exchange processes control tailing in the tracer washout curves, we propose a simple model that relates the late-time scaling to the distribution of vertical velocities at the sediment/water interface. Because vertical velocities drive advective pumping fluxes in and out of the streambed, we use a dimensional argument to suggest that the travel time distribution in the bed is inversely proportional to the distribution of interfacial vertical velocities: $t \sim 1/w$, where t is the time spent in the subsurface and w is the vertical component of velocity at the interface. The PDF for travel times can then be related to the velocity distribution:

$$p_t(t) = p_w(1/t)dw/dt = p_w(1/t) \cdot 1/t^2. \tag{1}$$

We extracted p_w from the velocity fields calculated by the spectral model, and compared the resulting predictions of p_t with the observed tailing in the washout curves.

Finally, we use the mobile-immobile transport model [*Schumer et al.*, 2003] with an initial condition in which the relatively immobile bed sediment is loaded with tracer. The solution, provided in the supplementary information, indicates that the power-law tailing in the washout curve reflects a power-law hyporheic residence time distribution with the same slope.

3. Results

Figure 1 shows the bed bathymetry for the smaller bedforms (top right) and for the larger bedforms (bottom right). The wavelengths and amplitudes of the bedforms generated under the higher flow were larger than those generated under the lower flow: 90 and

10 cm, respectively, for the larger bedforms versus 66 and 6 cm for the smaller bedforms [*Martin and Jerolmack*, 2013]. The tracer washout curves (Figure 1 left panel) indicate that both bed morphologies produced power law tailing that persisted throughout the 15 hours of observation of tracer concentrations. The power law slope of the washout curve was greater for solutes injected in the larger bedforms (exponent ≈ -1) than for solutes injected in the smaller bedforms (exponent ≈ -0.8). The washout curves obtained from particle tracking predicted exactly the scalings observed in the experimental washout data. Solute and elevation data can be downloaded from aubeneau.com/grl2015.

Figure 2 shows the power spectra of the bed elevation for both topographies. Both spectra show a typical white noise regime for scales larger than one wavelength (small wave-number). For smaller scales, the spectra reveal that the smaller topography spectrum has a smaller slope than the large topography spectrum, as indicated by their divergence between 1 and ~0.2 wavelengths. The behavior in this spatial scaling regime corresponds to the different scaling in time observed in the washout curves, and appears to control the residence time distribution in the bed. For smaller scales, both spectra show similar scaling. The intermediate topographic scaling for the smaller bedforms is that of a typical self-affine and self-similar Brownian walk described in many systems [*Turcotte*, 1997], whereas the larger bedforms exhibit greater longitudinal correlations, i.e., a smoother profile.

Figure 3 shows the probability distribution of vertical velocities at the sediment/water interface predicted using the particle tracking model and our simple analytical model. For the larger bedforms, $p_w(w) \sim 1/w$, which means that $p_t(t) \sim t * 1/t^2 \sim 1/t$, as observed in the tracer washout data (Figure 1). Likewise, for the smaller bedforms, $p_w(w) \sim 1/w^{1.2}$, which means that $p_t(t) \sim t^{1.2} * 1/t^2 \sim t^{-0.8}$, also as observed. The vertical velocities are higher for the large topography, indicating a higher hyporheic exchange with the bed. This is also consistent with the higher concentration of tracer in the washout curves tails for the large topography (visible from the raw data available online).

4. Discussion and conclusions

Our data show that the transit time distribution in a small sand-bed reach follows a power-law at late times. This behavior is clearly associated with hyporheic exchange, as it matches the scaling predicted by numerical particle-tracking simulations based on flow-topography interaction. Although others have observed tailing in headwater streams with high relief [*Haggerty et al.*, 2002], measuring late time tailing in fine sediments remains difficult due to the low tail concentrations resulting from in-stream injection experiments [*Drummond et al.*, 2012]. Our experimental setup allowed us to measure scaling in tracer washout over orders of magnitude of concentration and time. Our data confirm predictions of hyporheic exchange models based on streambed topographic spectra [*Worman et al.*, 2006; *Stonedahl et al.*, 2012] and indicate that the power-law timescale distribution can be directly related to vertical porewater flows, which can be extracted from topography. Using a mobile-immobile framework, we showed that the mobile zone washout curves resulting from loading the full streambed with tracer scales like the memory function (see supplementary information), meaning that the breakthrough curves scale as $t^{-\alpha}$ instead of $t^{-(\alpha+1)}$. The exponents are consistent with previous studies, although toward the higher end of known values [*Elliott and Brooks*, 1997; *Drummond et al.*, 2012]. This may be due to the type and scale of topographic features considered here, as other studies have usually considered steeper and larger headwater streams with larger bed roughness and friction. Our results suggest that higher exponents (under otherwise similar hydraulic regimes) are expected from smoother, more spatially correlated elevation profiles.

The power spectrum analysis indicates that the fractal properties of the topography are related to the transit time distribution in the system. The differences in fractal dimensions between the two topographies studied here reflected the differences observed in the breakthrough curves. Linking the time signature of processes happening on fractal objects to the fractality of the physical template is an old problem [*Wheatcraft and Tyler*, 1988] that remains a major theoretical challenge [*Shlesinger et al.*, 1993]. Many studies have proposed that diffusion on a fractal corresponds to fractional diffusion (i.e., power-law scaling in time), but to date there is no rigorous proof. However, increasing evidence from numerical experiments show that motion processes on fractals yield fractional signatures [*Reeves et al.*, 2008; *Harman et al.*, 2009]. Here, we showed directly that the fractality of streambed topography was related to the late-time scaling in the hyporheic residence time distribution.

The power spectrum of the elevation profiles gives information about the height of topographic features found at a given frequency. We observed that larger bedforms induced more hyporheic exchange but shorter residence times, as evidenced by the steeper slope of the washout curve. This is a key finding that is important for streams and rivers where large features are left behind by high flows. Such "frozen", "relict" features may therefore contribute disproportionately to the total exchange between surface and subsurface water, while also shortening the time water spends in the subsurface. This may be due to the higher aspect ratio of the larger topography (0.11 vs 0.09 for the small topography), which controls head gradient and therefore hyporheic exchange characteristics [*Worman et al.*, 2007]. In sand-bed rivers, morphology is fractal below a maximum bedform size controlled by finite size effects [*Nikora et al.*, 1997; *Jerolmack and Mohrig*, 2005]. These systems should therefore exhibit heavy-tailed residence time distributions and breakthrough curves. Moreover, as rivers generally have fractal topography [*Turcotte*, 1997] and surface-groundwater exchange is induced by all scales of topography, not just flow-bedform interaction [*Harvey and Bencala*, 1993], our findings may apply to other types of streams. Characterization of river-bed morphology along with hyporheic exchange and local vertical velocities and head gradients is therefore expected to enable new and more general assessment of surface-subsurface exchange processes.

In natural rivers, occasional high flows leave legacy topography behind that smaller flows will experience for long periods, since topography adjusts much faster to the rising flows than the recessions [*Martin and Jerolmack*, 2013]. *Patil et al.* [2012] showed that tail slopes of conservative tracer breakthrough curves in a mountain stream decreased at lower discharge. As the flow rises and intersects larger topographic features, the slope of the tails becomes steeper. Conversely, streams may experience wider retention distributions after the topography equilibrates with the smaller flows, as smaller topographies can delay flushing from the bed. These dynamic processes of flow-morphology interactions are crucial for characterizing solute transport and retention in river networks, but have yet to be incorporated in models and experiments because of the inherent challenges in observing and simulating time-varying processes in rivers.

Acknowledgments. The project was funded by NSF Grants EAR-0810270 and EAR-1215898. We thank the staff at SAFL for their help and support. The data for this paper is accessible at aubeneau.com/grl2015

References

Alexander, R. B., R. A. Smith, and G. E. Schwarz (2000), Effect of stream channel size on the delivery of nitrogen to the gulf of mexico, *Nature*, *403*(6771), 758–761.

Aubeneau, A., B. Hanrahan, D. Bolster, and J. L. Tank (2014), Substrate size and heterogeneity control anomalous transport in small streams, *Geophysical Research Letters*.

Aubeneau, A. F., J. D. Drummond, R. Schumer, D. Bolster, J. L. Tank, and A. I. Packman (2015), Effects of benthic and hyporheic reactive transport on breakthrough curves, *Freshwater Science*, *34*.

Battin, T. J., L. A. Kaplan, J. D. Newbold, and C. M. Hansen (2003), Contributions of microbial biofilms to ecosystem processes in stream mesocosms, *Nature*, *426*(6965), 439–442.

Battin, T. J., L. A. Kaplan, S. Findlay, C. S. Hopkinson, E. Marti, A. I. Packman, J. D. Newbold, and F. Sabater (2008), Biophysical controls on organic carbon fluxes in fluvial networks, *Nature Geoscience*, *1*(2), 95–100.

Boano, F., J. Harvey, A. Marion, A. Packman, R. Revelli, L. Ridolfi, and A. Wörman (2014), Hyporheic flow and transport processes: Mechanisms, models, and biogeochemical implications, *Reviews of Geophysics*.

Boulton, A. J., S. Findlay, P. Marmonier, E. H. Stanley, and H. M. Valett (1998), The functional significance of the hyporheic zone in streams and rivers, *Annual Review of Ecology and Systematics*, pp. 59–81.

Cardenas, M. B. (2007), Potential contribution of topography-driven regional groundwater flow to fractal stream chemistry: Residence time distribution analysis of tóth flow, *Geophysical Research Letters*, *34*(5).

Cardenas, M. B. (2008), Surface water-groundwater interface geomorphology leads to scaling of residence times, *Geophysical Research Letters*, *35*(8), L08,402.

Drummond, J., T. Covino, A. Aubeneau, D. Leong, S. Patil, R. Schumer, and A. Packman (2012), Effects of solute breakthrough curve tail truncation on residence time estimates: A synthesis of solute tracer injection studies, *Journal of Geophysical Research: Biogeosciences (2005–2012)*, *117*(G3).

Elliott, A. H., and N. H. Brooks (1997), Transfer of nonsorbing solutes to a streambed with bed forms: Laboratory experiments, *Water Resources Research*, *33*(1), 137–151, doi:10.1029/96WR02783.

Gomez-Velez, J. D., and J. W. Harvey (2014), A hydrogeomorphic river network model predicts where and why hyporheic exchange is important in large basins, *Geophysical Research Letters*, *41*(18), 6403–6412.

Haggerty, R., S. Wondzell, and M. Johnson (2002), Power-law residence time distribution in the hyporheic zone of a 2nd-order mountain stream, *Geophysical Research Letters*, *29*(13), doi:10.1029/2002GL014743.

Harman, C. J., M. Sivapalan, and P. Kumar (2009), Power law catchment-scale recessions arising from heterogeneous linear small-scale dynamics rid a-3538-2008 rid d-2036-2010, *Water Resources Research*, *45*, W09,404, doi:10.1029/2008WR007392.

Harvey, J. W., and K. E. Bencala (1993), The effect of streambed topography on surface-subsurface water exchange in mountain catchments, *Water Resources Research*, *29*(1), 89–98, doi:10.1029/92WR01960.

Jerolmack, D. J., and D. Mohrig (2005), A unified model for subaqueous bed form dynamics, *Water Resources Research*, *41*.

Kiel, B. A., and M. B. Cardenas (2014), Lateral hyporheic exchange throughout the mississippi river network, *Nature Geoscience*, *7*(6), 413–417.

Kirchner, J. W., X. H. Feng, and C. Neal (2000), Fractal stream chemistry and its implications for contaminant transport in catchments rid b-6126-2009, *Nature*, *403*(6769), 524–527, doi:10.1038/35000537.

Kirchner, J. W., X. Feng, and C. Neal (2001), Catchment-scale advection and dispersion as a mechanism for fractal scaling in stream tracer concentrations, *Journal of Hydrology*, *254*(1), 82–101.

Martin, R. L., and D. J. Jerolmack (2013), Origin of hysteresis in bedform response to unsteady flows, *Water Resources Research*.

Marzadri, A., D. Tonina, A. Bellin, and J. Tank (2014), A hydrologic model demonstrates nitrous oxide emissions depend on streambed morphology, *Geophysical Research Letters*, *41*(15), 5484–5491.

Nikora, V. I., A. N. Sukhodolov, and P. M. Rowinski (1997), Statistical sand wave dynamics in one directional water flows, *J. Fluid Mech.*, *351*, 17 39.

Patil, S., T. P. Covino, A. I. Packman, B. L. McGlynn, J. D. Drummond, R. A. Payn, and R. Schumer (2012), Intra-stream variability in solute transport: Hydrologic and geomorphic controls on solute retention, *Journal of Geophysical Research*.

Raymond, P. A., J. Hartmann, R. Lauerwald, S. Sobek, C. McDonald, M. Hoover, D. Butman, R. Striegl, E. Mayorga, C. Humborg, et al. (2013), Global carbon dioxide emissions from inland waters, *Nature*, *503*(7476), 355–359.

Reeves, D. M., D. A. Benson, and M. M. Meerschaert (2008), Transport of conservative solutes in simulated fracture networks: 1. synthetic data generation, *Water resources research*, *44*(5).

Rodriguez-Iturbe, I., and A. Rinaldo (2001), *Fractal River Basins: Chance and Self-Organization*, Cambridge University Press.

Scher, H., G. Margolin, R. Metzler, J. Klafter, and B. Berkowitz (2002), The dynamical foundation of fractal stream chemistry: The origin of extremely long retention times, *Geophysical Research Letters*, *29*(5), 5–1.

Schumer, R., D. A. Benson, M. M. Meerschaert, and B. Baeumer (2003), Fractal mobile/immobile solute transport rid a-5882-2008, *Water Resources Research*, *39*(10), 1296, doi:10.1029/2003WR002141.

Shlesinger, M. F., G. M. Zaslavsky, and J. Klafter (1993), Strange kinetics, *Nature*, *363*(6424), 31–37.

Stonedahl, S. H., J. W. Harvey, A. Wörman, M. Salehin, and A. I. Packman (2010), A multiscale model for integrating hyporheic exchange from ripples to meanders, *Water Resources Research*, *46*(12).

Stonedahl, S. H., J. W. Harvey, J. Detty, A. Aubeneau, and A. I. Packman (2012), Physical controls and predictability of stream hyporheic flow evaluated with a multiscale model, *Water Resources Research*, *48*, W10,513, doi:10.1029/2011WR011582.

Stonedahl, S. H., J. W. Harvey, and A. I. Packman (2013), Interactions between hyporheic flow produced by stream meanders, bars, and dunes, *Water Resources Research*, *49*(9), 5450–5461.

Tonina, D., and J. M. Buffington (2011), Effects of stream discharge, alluvial depth and bar amplitude on hyporheic flow in pool-riffle channels, *Water Resources Research*, *47*(8).

Toth, J. (1963), A theoretical analysis of groundwater flow in small drainage basins, *Journal of geophysical research*, *68*(16), 4795–4812.

Turcotte, D. L. (1997), *Fractals and chaos in geology and geophysics*, Cambridge university press.

Wheatcraft, S. W., and S. W. Tyler (1988), An explanation of scale-dependent dispersivity in heterogeneous aquifers using concepts of fractal geometry, *Water Resources Research*, *24*(4), 566–578.

Worman, A., A. I. Packman, L. Marklund, J. W. Harvey, and S. H. Stone (2006), Exact three-dimensional spectral solution to surface-groundwater interactions with arbitrary surface topography rid b-7085-2009, *Geophysical Research Letters*, *33*(7), L07,402, doi:

10.1029/2006GL025747.

Worman, A., A. I. Packman, L. Marklund, J. W. Harvey, and S. H. Stone (2007), Fractal topography and subsurface water flows from fluvial bedforms to the continental shield, *Geophysical Research Letters*, *34*(7), L07,402, doi:10.1029/2007GL029426.

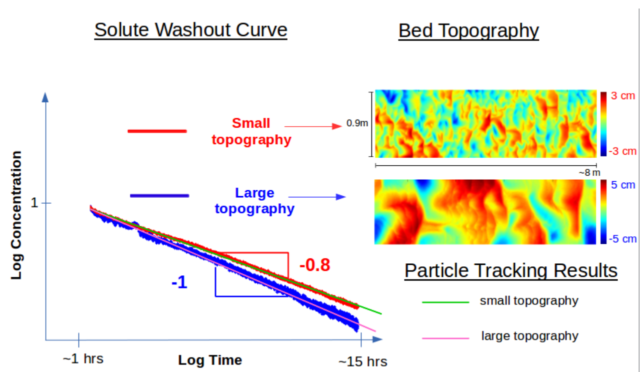

Figure 1. *Washout breakthrough curves measured under two contrasting streambed topographies.* Larger bedforms drove faster washout from the sand bed. Both topographies produced long-term ($\sim$ 15 hrs) power law tailing. The washout curves obtained from the particle tracking model agree well with the observations.

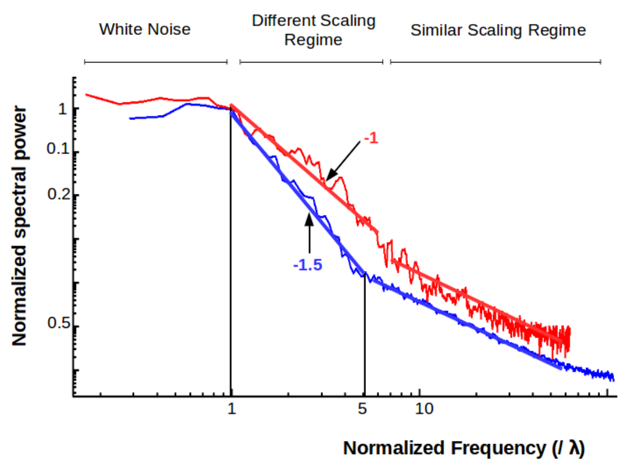

Figure 2. *Power spectra of streambed topographies.* The smaller and larger bedform fields exhibited different scaling between ~ 1 and ~ 0.2 wavelength (λ). The data are normalized by the wavelength, λ (x axis), and the power spectrum of λ (y axis). The thick lines emphasize trends in the scaling regimes.

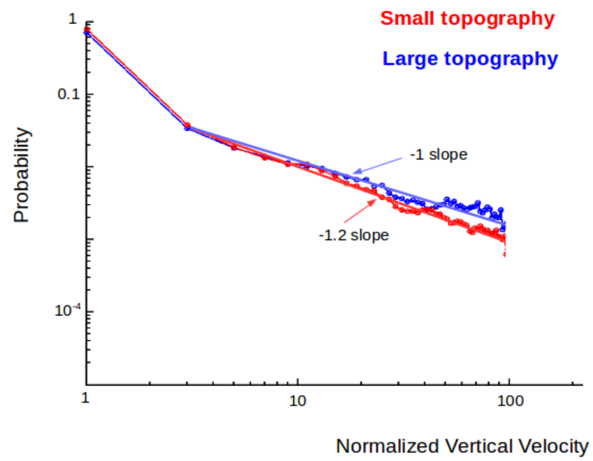

Figure 3. *Probability distribution of vertical velocities at the sediment/water interface.* The circles indicate results from the spectral model, while the solid lines indicate the slopes predicted from the theoretical relationship between the distribution of residence times and the distribution of vertical velocities. The vertical velocity distributions from both models match very well.